Style Equalization: Unsupervised Learning of Controllable Generative Sequence Models

Jen-Hao Rick Chang [1]   **Ashish Shrivastava** [1]   **Hema Swetha Koppula** [1]   **Xiaoshuai Zhang** [2]   **Oncel Tuzel** [1]

https://apple.github.io/ml-style-equalization

Abstract

Controllable generative sequence models with the capability to extract and replicate the style of specific examples enable many applications, including narrating audiobooks in different voices, auto-completing and auto-correcting written handwriting, and generating missing training samples for downstream recognition tasks. However, under an unsupervised-style setting, typical training algorithms for controllable sequence generative models suffer from the training-inference mismatch, where the same sample is used as content and style input during training but unpaired samples are given during inference. In this paper, we tackle the training-inference mismatch encountered during unsupervised learning of controllable generative sequence models. The proposed method is simple yet effective, where we use a style transformation module to transfer target style information into an unrelated style input. This method enables training using unpaired content and style samples and thereby mitigate the training-inference mismatch. We apply style equalization to text-to-speech and text-to-handwriting synthesis on three datasets. We conduct thorough evaluation, including both quantitative and qualitative user studies. Our results show that by mitigating the training-inference mismatch with the proposed style equalization, we achieve style replication scores comparable to real data in our user studies.

1. Introduction

The goal of controllable generative sequence models is to generate sequences containing target content in a target style. With the capability to select speaker voices, multi-speaker text-to-speech models have been successfully adopted in many voice assistants (Gibiansky et al., 2017; Ping et al., 2018; Hayashi et al., 2020). Many applications, however, require style controllability *beyond* selecting speaker voices. To perfectly reconstruct a speech example, we need to replicate not only the speaker's voice but also other aspects of style, including but not limited to prosody, intonation dynamics, background noise, echo, and microphone response appeared in the given sample. To utilize synthetic data to analyze failures or biases of a downstream recognizer, we need a style representation that models the style distribution beyond speaker identity. In these applications, style represents all information (except the content) to exactly reconstruct a sample, as illustrated in Fig. 1a. To model the temporal dynamics contained in input samples (*e.g.*, speech and handwriting), our style representation is a time-varying sequence, instead of a fixed vector. To capture the large variation of style, we learn the style representation in an *unsupervised* manner from a reference sample, rather than using a few human-annotated attributes.

Our goal is to learn a controllable generative sequence model that controls its style with a reference example (*e.g.*, an existing audio) and controls the content with a content sequence (*e.g.*, text), as shown in Fig. 1b. Our training dataset $\mathcal{X}$ is composed of $\left\{ (\mathbf{x}^i, \mathbf{c}^i) \right\}_{i=1,...,n}$, where $\mathbf{x}^i = \left[x_1^i \ \ldots \ x_{T_i}^i \,|\, x_t^i \in \mathbb{R}^d \right]$ is the i-th sample and $\mathbf{c}^i = \left[c_1^i \ \ldots \ c_{N_i}^i \,|\, c_j^i \in \mathbb{R}^m \right]$ is the corresponding content sequence. In general, $\mathbf{x}^i$ and $\mathbf{c}^i$ have different lengths, *i.e.*, $T_i \neq N_i$, and we do not assume to have the alignment between them. For example, in text-to-speech synthesis, $\mathbf{x}^i$ is the mel-spectrogram of an audio sample, $\mathbf{c}^i$ is the corresponding phonemes of the spoken words. While there exist methods, *e.g.*, (McAuliffe et al., 2017; Kotani et al., 2020), that can segment phonemes from an mel-spectrogram or characters from a handwriting sequence, we choose not to rely on these information and directly learn the alignment using attention. This allows the learned models to deal with ambiguous phoneme/character boundaries (*e.g.*, cursive handwriting). We also do not assume to have any style supervision, including speaker or attribute labels, nor any grouping of the data based on style.

[1] Apple [2] University of California, San Diego. Correspondence to: Jen-Hao Rick Chang <jenhao_chang@apple.com>.

(a) Style and content contain all information about a sample

(b) Controllable generative sequence model

(c) Training-inference mismatch leads to generation errors
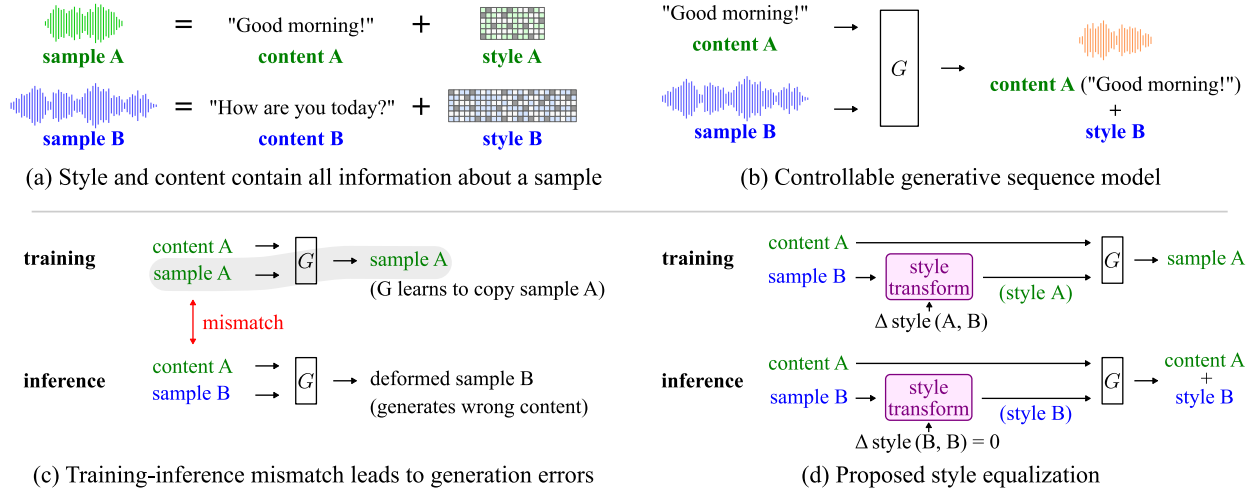
(d) Proposed style equalization

Figure 1: **Controllable generative models with sample-level style control.** (a) The information contained in a sample can be divided into content (*i.e.*, the text) and style (*i.e.*, all other information besides content). (b) Our goal during inference is to generate samples containing target content A in the style of sample B. Notice that sample B generally contains a different content. (c) There exists a training-inference mismatch when learning these models in typical unsupervised training of controllable generative models. During training, the *same* sample is used as content input and style input, whereas during inference, content and style inputs are from different samples, *i.e.*, the reference style sample contains a different content than the target content. The mismatch leads to incorrect content generation during inference. (d) To mitigate the training-inference mismatch, the proposed style equalization takes unpaired samples as input during both training and inference. It transforms the style of sample B to that of A by estimating their style difference.

While the unsupervised setting requires only the essential information (*i.e.*, samples and their content), it makes learning a controllable generative sequence model difficult. The main challenge is the mismatch between the inputs used during training and inference. As shown in Fig. 1c, during inference we pair arbitrary content A and reference sample B as inputs (*i.e.*, nonparallel setting). However, due to the lack of ground truth containing content A and in the style of B, during training we pair content A and sample A (*i.e.*, parallel setting). In other words, we train the model under the parallel setting but we use the model in the non-parallel setting during inference. Due to the training-inference mismatch, a well-performing model during training may perform poorly during inference. If a generative model learns to utilize the content information in the style example, during inference the generative model will generate wrong content. This phenomenon is called *content leakage* (Hu et al., 2020). In an extreme case, a model can learn to copy the reference sample to the output; despite its perfect training loss, it is useless because it always generates wrong content in practice.

This paper proposes a simple but effective technique to deal with the training-inference mismatch when we learn controllable auto-regressive models in an unsupervised-style manner. As shown in Fig. 1d, we train the model under the non-parallel setting, *i.e.*, we pair arbitrary content A with an arbitrary sample B from the training dataset. Instead of directly using sample B as style (in which case we have no

ground-truth output), we jointly learn a style transformation function, which estimates the style difference between A and B and transforms the style of sample B to the style of A. The generative model then takes content A and the transformation output (that contains the style of A and the unrelated content information from B) to reconstruct sample A. The proposed method enables us to use sample A as the ground truth while learning in the non-parallel setting—the intended usage during inference. Additionally, our method provides a systematic way to interpolate between the style of two samples by scaling the estimated style difference between two reference samples. We call the method *style equalization*. Note that for style equalization to work, the style transformation and difference estimator need to be carefully designed, such that no content information from content A can be transferred through sample B. We defer the discussion to Sec. 4.

We apply the proposed method on two signal domains, speech and online-handwriting, and evaluate the performance carefully via quantitative evaluation (by computing content error rates) and conducting qualitative user studies. Experimental results show that by tackling training-inference mismatch with the proposed style equalization, we are able to learn strong unsupervised controllable sequence generative models that have competitive performance even when compared to existing methods that utilize style supervision like speaker labels. On LibriTTS, style equalization

achieves close style replication (3.5 real oracle vs. 3.5 proposed in style opinion score) and content reproduction errors (6.6% real oracle vs. 9.5% proposed) to real samples.

2. Related Work

Controllable generative sequence models are not new in the literature; however, the majority of these methods utilize style supervision, whereas the paper focuses on developing an unsupervised-style method. Table 5 provides an overview of the related works.

Unsupervised-style methods. Unsupervised methods extract style information directly from samples, *i.e.*, without any style labels or pretrained style embeddings. Existing unsupervised methods train models under the parallel setting, as shown in Fig. 1c. To prevent content leakage, most existing methods introduce a bottleneck on the capacity of the style encoder by representing style as a single (time-invariant) vector and limiting its dimension (Wang et al., 2018; Hsu et al., 2018; Hu et al., 2020; Ma et al., 2018). Wang et al. (2018) propose Global Style Token (GST), which represents a style vector as a linear combination of a learned dictionary (called style tokens) shared across the dataset. The number of style tokens (the implicit dimension of the style vector) is carefully controlled to prevent content leakage. As we will see in Sec. 3, the bottleneck not only reduces the amount of content information contained in the style vector but also sacrifices style information.

Alternative loss formulations have also been proposed to limit content information contained in the style representation. Hu et al. (2020) minimize the mutual information between the style vector and the content sequence but requires a pretrained content encoder and adversarial learning, which makes training their model difficult. Hsu et al. (2018) approximate the posterior distribution of the style vector using a mixture of Gaussian distributions with a small number of mixtures. Ma et al. (2018) utilize a discriminator conditioned on both the generated output and the content (similar to a content recognizer). Akuzawa et al. (2018) anneal the Kullback-Leibler divergence to control the amount of information contained in style. Henter et al. (2018) utilize phoneme segmentation (McAuliffe et al., 2017) to avoid learning the alignment between content **c** and output **x**.

Priming is a technique that is introduced to control the style of auto-regressive generative sequence models (Graves, 2013; Aksan et al., 2018). Since the hidden state of a Recurrent Neural Network (RNN) contain all information about current generation, including style, we can initialize the RNN by pre-rolling the reference sample through the RNN. Utilizing priming requires the content of the reference style. For example, Aksan et al. (2018) learn a character recognizer and use it during inference. Moreover, since the hidden state contains residual content from the reference example, it often generates unexpected artifacts at the beginning of the sequence, as will be seen in Sec. 5.

Supervised-style methods. Many existing controllable generative models utilize style supervision, either directly by passing attribute labels as inputs or implicitly by grouping training data with their attribute labels. In the following, we briefly introduce various supervised controllable sequence models. While using style supervision avoids training-inference mismatch, it limits the style control on a few sparsely-defined attribute classes. For instance, given a speech audio, we can recognize the spoken texts, the accent, or even the speaker, but provided solely with these attribute labels, it is impossible to exactly reconstruct the original speech audio. The sparsely-defined attributes are insufficient to capture the entire style information.

User identifications or their embeddings have been used to learn multi-speaker text-to-speech models (Jia et al., 2018; Gibiansky et al., 2017; Kameoka et al., 2020; Donahue et al., 2020; Chen et al., 2021; Dhariwal et al., 2020; Valle et al., 2020; Kim et al., 2020; Hayashi et al., 2020; Sun et al., 2020b; Skerry-Ryan et al., 2018; Sun et al., 2020a), voice conversion models (Qian et al., 2019; Lee et al., 2021) and handwriting models (Kotani et al., 2020; Bhunia et al., 2021; Kang et al., 2020; Davis et al., 2020). In addition to user identifications, predefined features like pitch, phoneme duration, loudness, and timbre have also been used by existing methods (Ren et al., 2020; Qian et al., 2020; Dhariwal et al., 2020; Valle et al., 2020). Instead of using speaker labels as input, Kameoka et al. (2018); Kaneko & Kameoka (2018); Kaneko et al. (2019a;b) group training samples by their speaker labels and apply adversarial learning to learn voice conversion models that change speaker voices while keeping the content of the input.

Image methods. Controllable generative models have also been developed for images (Härkönen et al., 2020; Esser et al., 2019; Singh et al., 2019; Lample et al., 2017; Karras et al., 2020; Brock et al., 2019; Collins et al., 2020; Shen et al., 2020; Esser et al., 2020; Goetschalckx et al., 2019; Pavllo et al., 2020; Zhang et al., 2018; Chan et al., 2021; Kwon & Ye, 2021; Kazemi et al., 2019), which control the object class, pose, lighting, *etc.*, of an image. Many image style transform methods have also been developed (Isola et al., 2017; Zhu et al., 2017; Gatys et al., 2016; Kotovenko et al., 2019). However, there is a fundamental difference between image and sequence problems. In image generative models, we do not need to learn the content-output alignment. The content is usually defined globally as an image class or as pixel labels, *e.g.*, segmentation map. In contrast, our content is given as text, the output is mel-spectrogram of a waveform, and the content and output have different

lengths. To utilize the input content sequence, generative sequence models need to align the content and the output sequences and translate text to the output signal modality. The complication exacerbates the training-inference mismatch for sequence methods, since copying the style input is easier than utilizing the input content.

3. Controllable Generative Sequence Models

We focus on learning controllable auto-regressive generative models, $p(x_t|z_t, \mathbf{x}_{1..t-1}, \mathbf{c})$, where $\mathbf{x} = [x_1, \ldots, x_T]$ is the output sequence, $\mathbf{c}$ is the content sequence, and $\mathbf{z} = [z_1, \ldots, z_T \,|\, z_t \in \mathbb{R}^\ell]$ is the reference style information. Note that, in our model, style is also represented as a sequence that changes over time. Under the style-unsupervised setting, we are given a dataset $\mathcal{X} = \{(\mathbf{x}^i, \mathbf{c}^i), i \in \{1 \ldots n\}\}$ that contains the ground-truth output sequence $\mathbf{x}^i$ and the corresponding content $\mathbf{c}^i$, but we do not have supervision on $\mathbf{z}$. Therefore, we treat z_t as a latent variable with a learnable prior distribution $p(z_t|\mathbf{x}_{1..t-1}, \mathbf{c})$ and optimize the log-likelihood of $\mathbf{x}$ conditioned on $\mathbf{c}$, $\mathbb{E}_{(\mathbf{x},\mathbf{c})} \log p(\mathbf{x}|\mathbf{c})$.

Our model is a variational RNN (Chung et al., 2015), and we maximize a variational lower bound of the likelihood:

$$
\mathbb{E}_{(\mathbf{x},\mathbf{c})} \log p(\mathbf{x}|\mathbf{c}) = \mathbb{E}_{(\mathbf{x},\mathbf{c})} \sum_{t=1}^{T} \log p(x_t|\mathbf{x}_{1..t-1}, \mathbf{c})
$$

$$
= \mathbb{E}_{(\mathbf{x},\mathbf{c})} \sum_{t=1}^{T} \log \mathbb{E}_{z_t \sim p(z_t|\mathbf{x}_{1..t-1},\mathbf{c})} p(x_t|z_t, \mathbf{x}_{1..t-1}, \mathbf{c})
$$

$$
\geq \mathbb{E}_{(\mathbf{x},\mathbf{c})} \sum_{t=1}^{T} \mathbb{E}_{z_t \sim q(z_t|\mathbf{x},\mathbf{c})} \log p(x_t|z_t, \mathbf{x}_{1..t-1}, \mathbf{c})
$$

$$
- \mathcal{D}_{KL}\left(q(z_t|\mathbf{x},\mathbf{c}) \,||\, p(z_t|\mathbf{x}_{1..t-1},\mathbf{c})\right), \quad (1)
$$

where $\mathcal{D}_{KL}$ represents the Kullback-Leibler (KL)-divergence. In eq. (1), we use the chain rule to expand $p(\mathbf{x}|\mathbf{c})$ into $p(x_1|\mathbf{c})\,p(x_2|x_1,\mathbf{c})\cdots p(x_T|\mathbf{x}_{1..T-1},\mathbf{c})$, introduce the variational approximation $q(z_t|\mathbf{x},\mathbf{c})$ of the posterior distribution $p(z_t|\mathbf{x},\mathbf{c})$ for all t, and apply Jensen's inequality. Note that since q is a variation approximation of the posterior distribution, it can be conditioned on any variable. As we will see in Sec. 4, the proposed style equalization manipulates the input to q such that we condition q on a style-transformed unrelated sample $\mathbf{x}'$ instead of $\mathbf{x}$.

Fig. 2a shows an overview of the network used in the paper — the input content $\mathbf{c}$ is processed by the content attention, the style encoder (shown in green) models $q(z_t|\mathbf{x}^r, \mathbf{c})$, and the decoder (shown in gray) models $p(x_t|z_t, \mathbf{x}_{1..t-1}, \mathbf{c})$ using output from the style encoder and the content attention. Note that during inference, $\mathbf{x}^r$ is the reference example that we replicate the style of, and it generally contains an unrelated content, *i.e.*, $\mathbf{c}^r \neq \mathbf{c}$. During training, the ground-truth

sample $\mathbf{x}$ is used as the reference style to optimize eq. (1), *i.e.*, $\mathbf{x}^r = \mathbf{x}$ and $\mathbf{c}^r = \mathbf{c}$, which is different from inference. Therefore a generative model can learn to copy the style input to the output (and ignore the content input), leading to incorrect generation during inference. This phenomenon can be remedied by limiting the capacity of the style encoder, *e.g.*, by decreasing the dimensionality of the style representation. However, to achieve the lower bound of eq. (1) and hence a higher generation quality, we need the style encoder to contain enough capacity such that $q(z_t|\mathbf{x},\mathbf{c}) \equiv p(z_t|\mathbf{x},\mathbf{c})$ for all t. In this paper, we provide an alternative training procedure that bypasses this trade-off, allowing us to use a powerful style encoder (shown in Fig. 2b) with a high-dimensional style representation.

4. Style Equalization

Let $(\mathbf{x}, \mathbf{c})$ and $(\mathbf{x}', \mathbf{c}')$ be two samples from the training set. To match the inference setting, we should train the model using $\mathbf{c}$ as content and $\mathbf{x}'$ as style input. However, neither $\mathbf{x}$ nor $\mathbf{x}'$ can be used as the ground-truth output sequence. If we use $\mathbf{x}$ as the ground-truth output sequence but $\mathbf{x}'$ as style input, the generative model will learn to ignore the style encoder since $\mathbf{x}'$ contains unrelated style information. In other words, the variational approximation $q(\mathbf{z}|\mathbf{x}', \mathbf{c})$ is a poor approximation to the true posterior $p(\mathbf{z}|\mathbf{x}, \mathbf{c})$. Alternatively, if we use $\mathbf{x}'$ as the ground-truth output sequence, the content given in $\mathbf{c}$ will be ignored.

We introduce a learnable style transformation function $\mathcal{M}(\mathbf{x}', \delta)$ to transform the style of $\mathbf{x}'$ by the amount specified by a style difference vector $\delta \in \mathbb{R}^k$. We first estimate δ with a learnable function ϕ, *i.e.* $\delta = \phi(\mathbf{x}', \mathbf{x})$; we then transform $\mathbf{x}'$ with $\mathcal{M}(\mathbf{x}', \delta)$. By jointly optimizing $\mathcal{M}$, ϕ, and the rest of the generative model using eq. (1) (with the input to q modified as described), the model learns to transfer style information from $\mathbf{x}$ through $\mathcal{M}$ to maximize the log-likelihood of the ground-truth $\mathbf{x}$. In other words, we approximate the posterior distribution $p(\mathbf{z}|\mathbf{x}, \mathbf{c})$ with $q(\mathbf{z}|\mathcal{M}(\mathbf{x}', \phi(\mathbf{x}', \mathbf{x})), \mathbf{c})$, which is a better approximation than $q(\mathbf{z}|\mathbf{x}', \mathbf{c})$. We call this method *style equalization*.

Note that, for style equalization to be successful, $\mathcal{M} \circ \phi$ should not transfer any content-related information (*e.g.*, copy the entire sequence) from $\mathbf{x}$ but only its style information so that the decoder will utilize the transferred style and will rely on provided content input to generate the output. Therefore the design of $\mathcal{M}$ is critical.

Design of $\mathcal{M}$ and ϕ. An important observation we use in the design of $\mathcal{M}$ and ϕ is that content information (*i.e.*, sequence of phonemes or characters) is strongly time-dependent whereas the style can be reasonably well approximated by a time-independent representation (*e.g.*, voice characteristics of a speaker and microphone response, *etc.*).

(a) overview of the entire model

(b) proposed style encoder

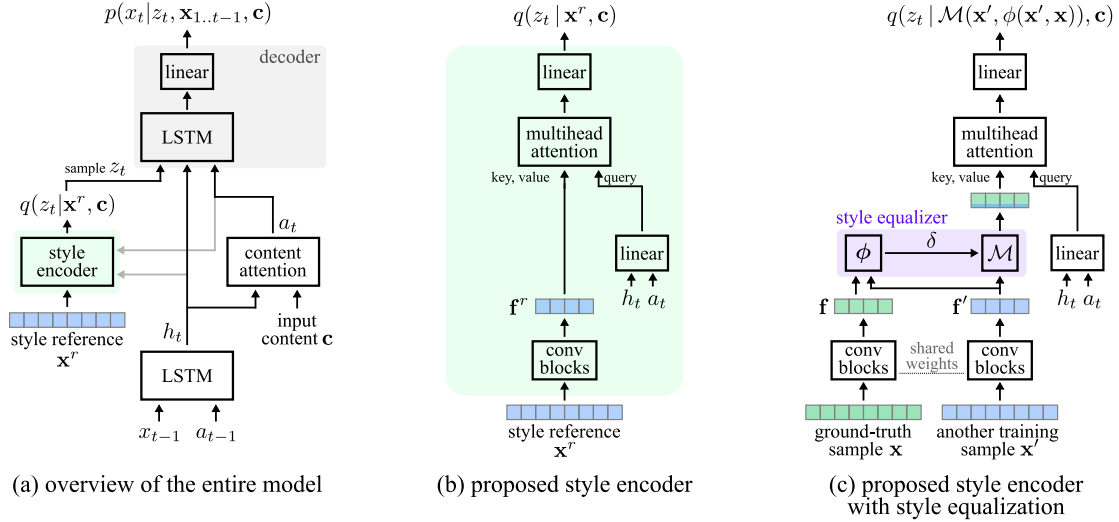(c) proposed style encoder with style equalization

Figure 2: **Model used in the paper.** (a) an overview of the entire model, which includes a style encoder (in green), content attention, and decoder (in gray). Note that the input content $\mathbf{c}$ can be the output of a content-embedding network (used in speech synthesis) or one-hot encoding of characters (used in handwriting synthesis). a_t is the output of the content attention at time t, which is a linear combination of the elements in $\mathbf{c}$. (b) the proposed style encoder without style equalization. (c) the proposed style encoder with the style equalization. ϕ computes the vector δ that encodes the style difference between $\mathbf{x}'$ and $\mathbf{x}$. $\mathcal{M}$ applies this transformation to $\mathbf{x}'$ to match the style of $\mathbf{x}$.

By designing ϕ such that no time-dependent information is stored in δ, we can satisfy that content-related information is not leaked but still transfer the time-independent style information. Thus, we utilize average pooling over the time dimension in ϕ, and to improve the time-invariant property of the convolutional network in our style encoder, we use convolutional filters without padding and with low-pass filtering before down-sampling (Zhang, 2019).

As shown in Fig. 2c, to estimate the style difference vector δ between two sequences $\mathbf{x}$ and $\mathbf{x}'$, we first compute their style features $\mathbf{f}$ and $\mathbf{f}'$ using a convolutional network. Note that $\mathbf{f}$ and $\mathbf{f}'$ are s-dimensional feature sequences with different lengths. We define

$$\phi(\mathbf{x}', \mathbf{x}) = \text{avg}(A\,\mathbf{f}) - \text{avg}(A\,\mathbf{f}') \text{ and}$$
$$\mathcal{M}(\mathbf{x}', \phi(\mathbf{x}', \mathbf{x})) = \mathbf{f}' + A^\top \phi(\mathbf{x}', \mathbf{x}), \quad (2)$$

where avg represents taking mean across time, $A \in \mathbb{R}^{k \times s}$ is a learnable linear transform, and $\mathbf{f}' + A^\top \phi(\mathbf{x}', \mathbf{x})$ means that the vector $A^\top \phi(\mathbf{x}', \mathbf{x}) \in \mathbb{R}^s$ is added to each time step of $\mathbf{f}'$. Intuitively, the design assumes that the style information lies on a k-dimensional subspace, and we equalize the style between $\mathbf{x}'$ and $\mathbf{x}$ by minimizing their differences in the subspace. It also satisfies the identity property by construction — $\phi(\mathbf{x}^r, \mathbf{x}^r) = 0$ and $\mathcal{M}(\mathbf{x}^r, 0) = \mathbf{f}^r$ — which enables style interpolation (see below) and allows us to treat style equalization as a training procedure and remove it from the model during inference (as shown in Fig. 2b). Note that making a convolutional network entirely time-invariant is an

important ongoing research problem (Karras et al., 2021); please see Sec. H for the discussions on our limitations.

Interpolation between two styles. Once learned, $\mathcal{M}$ and ϕ can be used to interpolate style during inference. Given two style references, $\mathbf{x}^s$ and $\mathbf{x}^t$, we interpolate between them with $\mathcal{M}(\mathbf{x}^s, \alpha\,\phi(\mathbf{x}^s, \mathbf{x}^t))$, where a scalar $\alpha \in \mathbb{R}$ controls the interpolation. By changing α, we traverse a one-dimensional manifold that starts from the original style (with $\alpha = 0$, since $\mathcal{M}(\mathbf{x}^s, \phi(\mathbf{x}^s, \mathbf{x}^s)) = \mathbf{f}^s$) and ends at the target style (with $\alpha = 1$). Note that, unlike existing generative models that support style interpolation in post-processing, $\mathcal{M}$ and ϕ are trained to transform style by design.

5. Experiments

To demonstrate the generality of the proposed method, we train and evaluate it on two signal domains, speech and handwriting, with the same model architecture design. In the following, we introduce the model architecture used in the experiments, the baselines, the metrics, and the results. More details are provided in Sec. C.

5.1. Model Architecture

Our model is auto-regressive and composed of (i) a decoder that is modeling $p(x_t|z_t, \mathbf{x}_{1..t-1}, \mathbf{c})$, (ii) a content attention module, (iii) a style encoder that is modeling $q(z_t|\cdot, \mathbf{c})$, and (iv) a network that models the prior distribution of z_t. Fig. 2a shows an overview of the model. The backbone of the

model, namely the content attention and the decoder, uses a standard architecture that was proposed by Graves (2013) for handwriting synthesis and later extended to speech in variations of Tacotron (Shen et al., 2018; Wang et al., 2018). The variational approximation $q(z_t|\cdot)$ and the prior distribution are modeled as multivariate Gaussian distributions with a diagonal covariance matrix.

Our style encoder is composed of a convolutional network and a multi-head attention layer, as shown in Fig. 2b. The convolutional network extracts the style feature sequence $\mathbf{f}^r$ from the reference style input $\mathbf{x}^r$. We use multi-head attention to extract relevant style information at every time step from $\mathbf{f}^r$ with the query computed from the hidden state of the LSTM, h_t, which contains information about past generations, and the currently focused content a_t. Thus, while δ contains only time-invariant information, our style representation is a time-varying sequence. The intuition is if the model utters a particular phoneme, it should be able to find the information in the style reference and mimic it.

For style equalization, we insert $\mathcal{M}$ and ϕ into the style encoder, as shown in Fig. 2c. Since style equalization is only able to transfer time-independent information, when we utilize this procedure, the network will not be able to learn time-dependent style. To enable learning time-dependent style information during training, half of the batches, we use $\mathbf{x}' = \mathbf{x}$, which means that the difference vector $\delta = 0$, hence the decoder directly uses the ground-truth style information which contains time-dependent style information. We analyze the effect of style attention and its ability to represent time-varying style information in Sec. 5.4.

5.2. Speech Synthesis

We train and evaluate the proposed method on two multi-speaker speech datasets. VCTK dataset (Yamagishi et al., 2019) contains 110 speakers and 44 hours of speech, and LibriTTS dataset (Zen et al., 2019) contains 2,311 speakers and 555 hours of speech in the training set.

Baselines. We compare the proposed method with Global Style Tokens (GST-n) (Wang et al., 2018) with various numbers of tokens n. For completeness, we also compare with Tacotron 2 (Shen et al., 2018) (even though it does not have style control), Tacotron-S and GST-nS. Tacotron-S / GST-nS are Tacotron / GST-n with style supervision — a pretrained speaker embedding (Snyder et al., 2018) that was trained on the VoxCeleb dataset, which contains $2,000$ hours of speech from $7,000$ speakers (Chung et al., 2018). We use ESPnet-TTS (Hayashi et al., 2020), a widely used implementation of the baselines and follow their training recipe. They achieve similar performance as those listed in the original papers. With no publicly available implementation, we cannot compare with (Hsu et al., 2018) and (Ma et al.,

Table 1: Quantitative results on VCTK dataset. The reference style inputs are seen (randomly selected from the training set). WER measures content accuracy; cosine-similarity (cos-sim) and sRank measure style similarity.

Method	Parallel text			Nonparallel text		
	WER (%)	cos-sim ↑	sRank ↓	WER (%)	cos-sim ↑	sRank ↓
Tacotron	16.0 ± 1.7	0.05 ± 0.13	53.1 ± 29.1	16.4 ± 1.2	0.05 ± 0.12	53.9 ± 27.8
Tacotron-S	13.6 ± 0.7	0.24 ± 0.18	16.4 ± 20.9	16.3 ± 0.4	0.22 ± 0.18	18.0 ± 21.9
GST-16	18.6 ± 0.9	0.23 ± 0.15	21.4 ± 21.9	18.5 ± 1.1	0.23 ± 0.16	21.1 ± 22.4
GST-64	16.9 ± 0.5	0.23 ± 0.17	24.4 ± 23.1	27.5 ± 0.4	0.22 ± 0.16	25.2 ± 24.4
GST-16S	8.3 ± 0.1	0.34 ± 0.18	10.8 ± 15.2	17.7 ± 0.8	0.31 ± 0.17	13.0 ± 20.0
GST-64S	14.1 ± 0.3	0.33 ± 0.18	11.4 ± 16.3	24.7 ± 1.0	0.32 ± 0.18	12.7 ± 18.1
Proposed	$\mathbf{7.4 \pm 0.2}$	$\mathbf{0.73 \pm 0.12}$	$\mathbf{1.5 \pm 2.1}$	$\mathbf{9.5 \pm 0.4}$	$\mathbf{0.64 \pm 0.14}$	$\mathbf{1.9 \pm 4.2}$
Oracle	6.6 ± 0.0	1.0 ± 0.0	1.0 ± 0.0	6.6 ± 0.0	0.57 ± 0.16	1.6 ± 4.1

2018). All methods are trained on the same dataset, while Tacotron-S and GST-nS have additional style supervision from VoxCeleb dataset. All methods output 80-dimensional mel-spectrograms with the sampling rate equal to 22,050 Hz and the window size equal to 1,024, which are converted to waveforms using a pretrained WaveGlow vocoder (Prenger et al., 2019). The content input is represented as phonemes, following (Shen et al., 2018).

Metrics. We measure the content generation errors as Word Error Rate (WER), using a pretrained speech recognition model, ESPnet (kamo naoyuki, 2021). To evaluate the style replication accuracy of the methods, we use a speaker classification network (Deng et al., 2019) (see Sec. D) and measure the style similarity between reference and output generations. We report cos-sim, which is the cosine similarity between the reference example and its corresponding output generation, and sRank, which is the rank of the reference speaker out of all speakers based on their cosine similarities. We report the empirical mean and standard deviation of these metrics on 100 pairs of reference and synthetic samples.

We also report the style opinion score following the protocol used by Zhao et al. (2020). To evaluate the style similarity between a generated output and a style reference, users were given pairs of reference and synthesized audio, and asked if "the two samples could have been produced by the same speaker in a similar environmental condition", and asked to score with " 4 (Absolutely same)", "3 (Likely same)", "2 (Likely different)", "1 (Absolutely different)". We synthesized 100 samples using each method with the same style example and target content. A total of 15 users participated in the study, and we collected 630 responses.

We also provide an oracle (a pseudo upper-bound) where we select a different real speech sample from the same speaker from the dataset, and evaluate style similarity and content error. This provides a good calibration for our evaluation metrics and opinion studies.

Table 2: Quantitative results on LibriTTS-all-960 dataset.

Method	Seen speakers, parallel text			Seen speakers, nonparallel text			Unseen speakers, nonparallel text		
	WER (%)	cos-sim ↑	sRank ↓	WER (%)	cos-sim ↑	sRank ↓	WER (%)	cos-sim ↑	sRank ↓
Tacotron	64.4 ± 4.1	0.00 ± 0.10	1218 ± 671	52.2 ± 1.7	0.01 ± 0.10	1140 ± 651	52.2 ± 0.6	0.00 ± 0.10	847 ± 563
Tacotron-S	14.9 ± 0.0	0.23 ± 0.22	430 ± 584	18.7 ± 0.2	0.24 ± 0.22	370 ± 562	13.5 ± 0.0	0.16 ± 0.16	289 ± 436
GST-64	38.2 ± 2.2	0.12 ± 0.19	706 ± 701	33.3 ± 3.4	0.12 ± 0.19	700 ± 739	30.4 ± 2.2	0.09 ± 0.16	535 ± 610
GST-192	19.3 ± 0.3	0.10 ± 0.17	786 ± 725	17.8 ± 0.6	0.09 ± 0.16	823 ± 719	18.0 ± 0.7	0.07 ± 0.14	587 ± 582
GST-64S	19.7 ± 0.7	0.39 ± 0.23	150 ± 305	20.4 ± 1.6	0.40 ± 0.23	143 ± 334	16.5 ± 0.2	0.28 ± 0.17	121 ± 259
GST-192S	13.8 ± 0.7	0.39 ± 0.23	137 ± 309	15.4 ± 1.1	0.41 ± 0.22	126 ± 317	13.4 ± 0.2	0.29 ± 0.18	139 ± 316
Proposed	$\mathbf{6.2 \pm 0.5}$	$\mathbf{0.82 \pm 0.14}$	$\mathbf{1.7 \pm 4.1}$	$\mathbf{9.4 \pm 0.3}$	$\mathbf{0.78 \pm 0.14}$	$\mathbf{1.8 \pm 6.0}$	$\mathbf{7.6 \pm 0.9}$	$\mathbf{0.57 \pm 0.15}$	$\mathbf{7.4 \pm 42.6}$
Oracle	6.5 ± 0.0	1.0 ± 0.0	1.0 ± 0.0	6.5 ± 0.0	0.85 ± 0.06	1.0 ± 0.0	6.5 ± 0.0	0.50 ± 0.23	3.6 ± 24.9

Table 3: Style opinion scores of speech synthesizers.

VCTK, seen speakers				LibriTTS, seen speakers				LibriTTS, unseen speakers			
GST-64	GST-16S	Proposed	Oracle	GST-192	GST-192S	Proposed	Oracle	GST-192	GST-192S	Proposed	Oracle
2.1 ± 1.0	3.3 ± 0.9	3.8 ± 0.4	3.8 ± 0.4	1.4 ± 0.6	2.8 ± 1.0	$\mathbf{3.6 \pm 0.6}$	3.5 ± 0.9	1.2 ± 0.5	2.6 ± 0.9	$\mathbf{3.5 \pm 0.7}$	3.5 ± 0.9

Results. Table 1 shows the results on VCTK dataset. Let us first look at the parallel-text setting. Without any style control, Tacotron achieves a low cosine similarity. Utilizing GST and speaker embedding (Tacotron-S and GST-nS) improve cosine similarities. With the proposed style equalization and the style encoder, our model achieves the highest similarity and lowest sRank.

When comparing the WERs between the parallel and nonparallel settings, we can see the adversarial effect of content leakage — the models with a high-capacity style encoder (GST-64, GST-16S, and GST-64S) produce a much higher word-error rate in the non-parallel setting than in the parallel setting, while the small capacity GST-16 is largely unaffected. In comparison, our model is less affected by the parallel / nonparallel settings. The supplemental website shows the generated audios.

Table 2 shows the results on LibriTTS dataset. As can be seen from the results, the large variety (*e.g.*, more accents, higher background noise, difficult microphone effects) makes it a more difficult dataset than VCTK, as reflected by the higher WERs of Tacotron than those in VCTK. The proposed method, on the other hand, is able to learn from the noisy data and mimic the wide variety of styles in the dataset. In addition, since the training set contains more than $2,000$ speakers, the proposed method learns to generalize and mimic the voices of unseen speakers in the validation set, as demonstrated by the high cosine similarity in the right-most column of Table 2. The supplemental website shows the generated audios, including those by a model using the same architecture as ours but trained without style equalization. While the model performs well in the parallel setting, it fails to generate the correct content in the non-parallel setting, and we can clearly hear the content from the nonparallel style input leaked into the generated output. In comparison, utilizing style equalization during training

significantly improves the problem. Please also see the supplemental website for results with style sampled from the prior distribution or interpolated between two examples.

Table 3 shows style opinion scores on the two datasets. The proposed method achieves high scores, similar to those of the oracle.

Finally, it is worth noting that by directly mimicking the reference style example, our models achieve higher or comparable cos-sim and style opinion scores in Table 1-3 than the oracle, which is a random sample in the dataset from the same speaker. These results indicate the effectiveness of mimicking the style of the given reference example over utilizing speaker embedding, which learns a generic voice of a speaker.

5.3. Online-Handwriting Synthesis

Online-handwriting synthesis aims to generate sequences of pen movements on a writing surface. A handwriting sample is represented as a sequence of (x, y, p) triplets, where x and y are the coordinates of the pen on the surface, and p is a binary variable indicating whether the pen touches the surface over time. We apply the proposed method to a subset of a proprietary dataset collected for research and development. The subset consists of 600k online handwriting samples that were written by 1,500 people in English, French, German, Italian, Spanish, and Portuguese.

Baselines and metrics. While there exist many handwriting synthesizers, most of them requires writer labels (Kotani et al., 2020; Bhunia et al., 2021; Kang et al., 2020) or character segmentation (Davis et al., 2020; Aksan et al., 2018; Kotani et al., 2020) (Table 5). We compare with the method proposed by Graves (2013) that uses priming for style encoding; since the proposed style equalization is a training mechanism, we also compare with an ablation of our model
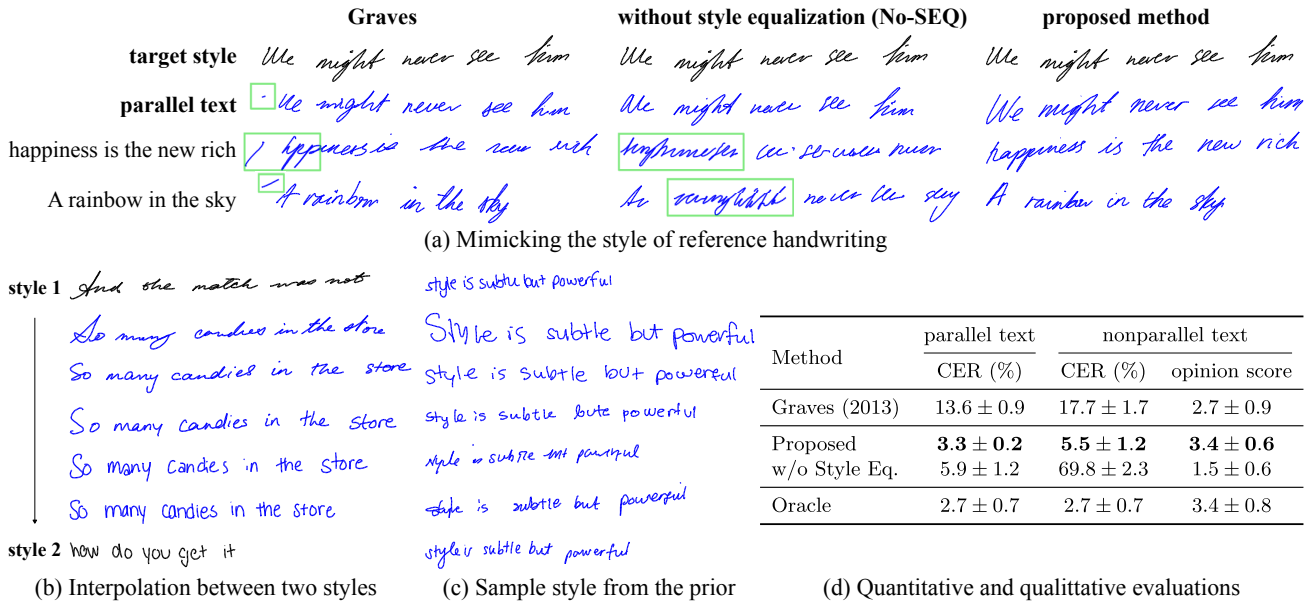
(a) Mimicking the style of reference handwriting

(b) Interpolation between two styles   (c) Sample style from the prior

Method	parallel text	nonparallel text	
	CER (%)	CER (%)	opinion score
Graves (2013)	13.6 ± 0.9	17.7 ± 1.7	2.7 ± 0.9
Proposed	$\mathbf{3.3 \pm 0.2}$	$\mathbf{5.5 \pm 1.2}$	$\mathbf{3.4 \pm 0.6}$
w/o Style Eq.	5.9 ± 1.2	69.8 ± 2.3	1.5 ± 0.6
Oracle	2.7 ± 0.7	2.7 ± 0.7	3.4 ± 0.8

(d) Quantitative and qualittative evaluations

Figure 3: **Handwriting generation results and evaluation.** The reference style examples are shown in black, and the outputs are shown in blue.

trained *without* style equalization. Note that all these models use the same decoder and content attention. Similar to speech, we measure content generation error as Character Error rate (CER) with a pretrained handwriting recognizer, and we conduct style-opinion-score study on 12 users and collected 320 responses. We also provide an oracle where we select a different real handwriting sample from the same writer from the dataset and compute the metrics.

Results. Fig. 3 shows synthesized handwriting from each of the methods on unseen style examples. As can be seen, while Graves (2013) with priming is an effective method to replicate the reference style, it often outputs artifacts at the beginning due to the residual information in the hidden state. The model without style equalization produces high-quality replication in the parallel setting; however, it suffers severely under the nonparallel setting and produces wrong content. By training with the proposed style equalization, the CER in the nonparallel setting improved significantly. We demonstrate style interpolate in Fig. 3b and results with styles sampled from the learned prior distribution in Fig. 3c.

Note that due to privacy reasons, the handwriting reference examples shown in the paper and the supplemental website are synthetic. They are close reproductions of unseen real styles using a generative model with a different architecture. The generations shown here are very similar when real samples are used as style input. All evaluations reported in Fig. 3d use real unseen style examples.

(a) 100%, $\mathbf{c}^r = \mathbf{c}$ (b) 50%, $\mathbf{c}^r = \mathbf{c}$

(c) 50%, $\mathbf{c}^r \neq \mathbf{c}$ (d) 50%, $\mathbf{c}^r = \mathbf{c}$, $\mathbf{x}^r$ transformed
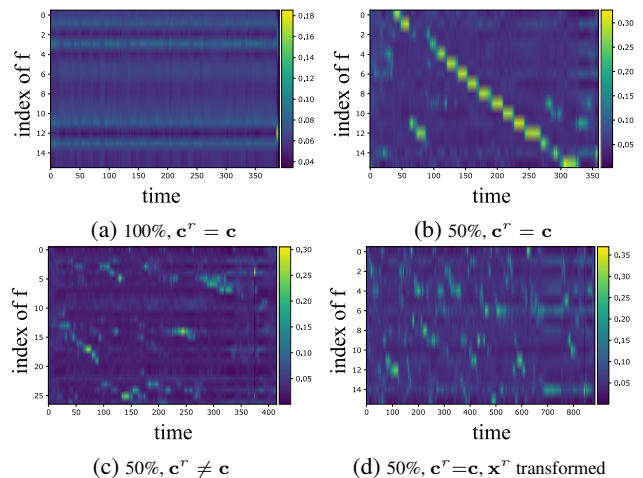
Figure 4: Style attention weights of two models trained on LibriTTS during inference on unseen styles. (a) style equalization always applied during training (100%) and (b,c,d) style equalization applied to 50% of the batches. All share the same input content $\mathbf{c}$, (a,b,d) share the same input style, but (d) transforms the input style to that of (c).

5.4. Analysis of Style Attention

Finally, we analyze how our model utilizes the time-dependent style information contained in the reference example $\mathbf{x}^r$ by examining the attention weights of the style attention module. As discussed in Sec. 4, while our style representation is a time-dependent sequence, style equalization can only transfer time-independent global style information

from the style reference. Therefore, when we apply style equalization to all the samples during training, we learn a time-independent representation. This can be seen from Fig. 4a where the attention weights become constant over time during inference.

We encourage our style encoder to learn the time-dependent aspects of style by applying style equalization only to 50% of the training samples. As can be seen from the time-varying attention weights in Fig. 4b-d, this training procedure enables the style encoder to utilize style information more efficiently by focusing time instances with similar signal and context. For example, when the style reference contains the target content, *i.e.*, $\mathbf{c}^r = \mathbf{c}$ (Fig. 4b), the attention weights form a block-diagonal pattern, indicating the model focuses to the time instances of the style signal that match the current content and context. When $\mathbf{c}^r \neq \mathbf{c}$ (Fig. 4c), the weights are still well localized over time to gather pieces of time-dependent style information from matching signal in $\mathbf{x}^r$. Last, we transform the parallel style (Fig. 4b) to that of a nonparallel one (Fig. 4c) during inference in Fig. 4d. Comparing Fig. 4b & d, the diagonal shape disappears, indicating the style transform reduces the source content information.

The flexibility to apply/remove style equalization (and hence the representation bottleneck) during training is one of the main differences compared to (Wang et al., 2018; Hsu et al., 2018), which always apply the style bottleneck.

6. Conclusion

This paper proposes a simple but effective training strategy, style equalization, to mitigate the training-inference mismatch and learn a generative sequence model where style and content can be controlled separately without utilizing any style supervision. We demonstrate 1) replication of styles from a single style reference, 2) interpolation between two reference styles, and 3) generating new styles. Experiments on both speech and handwriting domains show the effectiveness of the proposed method in mitigating the training-inference mismatch, which enables our models to obtain high-quality synthesis results.

References

Aksan, E., Pece, F., and Hilliges, O. Deepwriting: Making digital ink editable via deep generative modeling. In *Conference on Human Factors in Computing Systems (CHI)*, pp. 1–14, 2018.

Akuzawa, K., Iwasawa, Y., and Matsuo, Y. Expressive speech synthesis via modeling expressions with variational autoencoder. In *Interspeech*, 2018.

Alegre, F., Amehraye, A., and Evans, N. Spoofing countermeasures to protect automatic speaker verification from voice conversion. In *2013 IEEE International Conference on Acoustics, Speech and Signal Processing*, pp. 3068–3072. IEEE, 2013.

Bhunia, A. K., Khan, S., Cholakkal, H., Anwer, R. M., Khan, F. S., and Shah, M. Handwriting transformers. *arXiv preprint arXiv:2104.03964*, 2021.

Brock, A., Donahue, J., and Simonyan, K. Large scale GAN training for high fidelity natural image synthesis. In *International Conference on Learning Representations (ICLR)*, 2019.

Brundage, M., Avin, S., Clark, J., Toner, H., Eckersley, P., Garfinkel, B., Dafoe, A., Scharre, P., Zeitzoff, T., Filar, B., et al. The malicious use of artificial intelligence: Forecasting, prevention, and mitigation. *arXiv preprint arXiv:1802.07228*, 2018.

Chan, E. R., Monteiro, M., Kellnhofer, P., Wu, J., and Wetzstein, G. pi-GAN: Periodic implicit generative adversarial networks for 3D-aware image synthesis. In *IEEE Conference on Computer Vision and Pattern Recognition (CVPR)*, pp. 5799–5809, 2021.

Chen, M., Tan, X., Li, B., Liu, Y., Qin, T., sheng zhao, and Liu, T.-Y. AdaSpeech: Adaptive text to speech for custom voice. In *International Conference on Learning Representations (ICLR)*, 2021.

Chen, T., Kumar, A., Nagarsheth, P., Sivaraman, G., and Khoury, E. Generalization of audio deepfake detection. In *Proc. Odyssey 2020 The Speaker and Language Recognition Workshop*, pp. 132–137, 2020.

Chung, J., Kastner, K., Dinh, L., Goel, K., Courville, A. C., and Bengio, Y. A recurrent latent variable model for sequential data. *Advances in Neural Information Processing Systems (NeurIPS)*, 2015.

Chung, J. S., Nagrani, A., and Zisserman, A. VoxCeleb2: Deep speaker recognition. *Proc. Interspeech*, pp. 1086–1090, 2018.

Collins, E., Bala, R., Price, B., and Susstrunk, S. Editing in style: Uncovering the local semantics of GANs. In *IEEE Conference on Computer Vision and Pattern Recognition (CVPR)*, 2020.

Davis, B., Tensmeyer, C., Price, B., Wigington, C., Morse, B., and Jain, R. Text and style conditioned GAN for generation of offline handwriting lines. In *British Machine Vision Conference (BMVC)*, 2020.

Deng, J., Guo, J., Xue, N., and Zafeiriou, S. Arcface: Additive angular margin loss for deep face recognition. In *IEEE Conference on Computer Vision and Pattern Recognition (CVPR)*, 2019.

Dhariwal, P., Jun, H., Payne, C., Kim, J. W., Radford, A., and Sutskever, I. Jukebox: A generative model for music. *arXiv preprint arXiv:2005.00341*, 2020.

Dolhansky, B., Bitton, J., Pflaum, B., Lu, J., Howes, R., Wang, M., and Canton Ferrer, C. The deepfake detection challenge dataset. *arXiv e-prints*, pp. arXiv–2006, 2020.

Donahue, J., Dieleman, S., Bińkowski, M., Elsen, E., and Simonyan, K. End-to-end adversarial text-to-speech. *arXiv preprint arXiv:2006.03575*, 2020.

Esser, P., Haux, J., and Ommer, B. Unsupervised robust disentangling of latent characteristics for image synthesis. In *IEEE International Conference on Computer Vision (ICCV)*, 2019.

Esser, P., Rombach, R., and Ommer, B. A disentangling invertible interpretation network for explaining latent representations. In *IEEE Conference on Computer Vision and Pattern Recognition (CVPR)*, June 2020.

Evans, N. W., Kinnunen, T., and Yamagishi, J. Spoofing and countermeasures for automatic speaker verification. In *Interspeech*, pp. 925–929, 2013.

Gatys, L., Ecker, A., and Bethge, M. A neural algorithm of artistic style. *Journal of Vision*, 16(12):326–326, 2016.

Gibiansky, A., Arik, S., Diamos, G., Miller, J., Peng, K., Ping, W., Raiman, J., and Zhou, Y. Deep voice 2: Multi-speaker neural text-to-speech. In *Advances in Neural Information Processing Systems (NeurIPS)*, pp. 2966–2974, 2017.

Goetschalckx, L., Andonian, A., Oliva, A., and Isola, P. GANalyze: Toward visual definitions of cognitive image properties. In *IEEE International Conference on Computer Vision (ICCV)*, 2019.

Graves, A. Generating sequences with recurrent neural networks. *arXiv preprint arXiv:1308.0850*, 2013.

Güera, D. and Delp, E. J. Deepfake video detection using recurrent neural networks. In *2018 15th IEEE international conference on advanced video and signal based surveillance (AVSS)*, pp. 1–6. IEEE, 2018.

Härkönen, E., Hertzmann, A., Lehtinen, J., and Paris, S. GANSpace: Discovering interpretable GAN controls. In *Advances in Neural Information Processing Systems (NeurIPS)*, 2020.

Hayashi, T., Yamamoto, R., Inoue, K., Yoshimura, T., Watanabe, S., Toda, T., Takeda, K., Zhang, Y., and Tan, X. Espnet-TTS: Unified, reproducible, and integratable open source end-to-end text-to-speech toolkit. In *IEEE International Conference on Acoustics, Speech and Signal Processing(ICASSP)*, 2020.

Hendrycks, D. and Gimpel, K. Gaussian error linear units (gelus). *arXiv preprint arXiv:1606.08415*, 2016.

Henter, G. E., Lorenzo-Trueba, J., Wang, X., and Yamagishi, J. Deep encoder-decoder models for unsupervised learning of controllable speech synthesis. *arXiv preprint arXiv:1807.11470*, 2018.

Hsu, W.-N., Zhang, Y., Weiss, R. J., Zen, H., Wu, Y., Wang, Y., Cao, Y., Jia, Y., Chen, Z., Shen, J., et al. Hierarchical generative modeling for controllable speech synthesis. In *International Conference on Learning Representations (ICLR)*, 2018.

Hu, T.-Y., Shrivastava, A., Tuzel, O., and Dhir, C. Unsupervised style and content separation by minimizing mutual information for speech synthesis. In *IEEE International Conference on Acoustics, Speech and Signal Processing(ICASSP)*, 2020.

Hua, G., Huang, J., Shi, Y. Q., Goh, J., and Thing, V. L. Twenty years of digital audio watermarking — a comprehensive review. *Signal processing*, 128:222–242, 2016.

Hutchinson, M. F. A stochastic estimator of the trace of the influence matrix for laplacian smoothing splines. *Communications in Statistics-Simulation and Computation*, 18(3):1059–1076, 1989.

Islam, M. A., Jia, S., and Bruce, N. D. How much position information do convolutional neural networks encode? In *International Conference on Learning Representations (ICLR)*, 2019.

Isola, P., Zhu, J.-Y., Zhou, T., and Efros, A. A. Image-to-image translation with conditional adversarial networks. In *IEEE Conference on Computer Vision and Pattern Recognition (CVPR)*, pp. 1125–1134, 2017.

Jia, Y., Zhang, Y., Weiss, R. J., Wang, Q., Shen, J., Ren, F., Chen, Z., Nguyen, P., Pang, R., Moreno, I. L., et al. Transfer learning from speaker verification to multispeaker text-to-speech synthesis. In *Advances in Neural Information Processing Systems (NeurIPS)*, pp. 4485–4495, 2018.

Kameoka, H., Kaneko, T., Tanaka, K., and Hojo, N. StarGAN-VC: Non-parallel many-to-many voice conversion using star generative adversarial networks. In *Spoken Language Technology Workshop (SLT)*, pp. 266–273. IEEE, 2018.

Kameoka, H., Huang, W.-C., Tanaka, K., Kaneko, T., Hojo, N., and Toda, T. Many-to-many voice transformer network. *IEEE/ACM Transactions on Audio, Speech, and Language Processing*, 2020.

kamo naoyuki. ESPnet2 pretrained model, kamo-naoyuki/librispeech_asr_train_asr_conformer6_

n_fft512_hop_length256_raw_en_bpe5000_scheduler_confwarmup_steps40000_optim_conflr0.0025_sp_valid.acc.ave,fs=16k,lang=en, March 2021. URL https://doi.org/10.5281/zenodo.4604066.

Kaneko, T. and Kameoka, H. CycleGAN-VC: Non-parallel voice conversion using cycle-consistent adversarial networks. In *European Signal Processing Conference (EU-SIPCO)*, pp. 2100–2104. IEEE, 2018.

Kaneko, T., Kameoka, H., Tanaka, K., and Hojo, N. CycleGAN-VC2: Improved cycleGAN-based non-parallel voice conversion. In *IEEE International Conference on Acoustics, Speech and Signal Processing(ICASSP)*, pp. 6820–6824. IEEE, 2019a.

Kaneko, T., Kameoka, H., Tanaka, K., and Hojo, N. StarGAN-VC2: Rethinking conditional methods for starGAN-based voice conversion. In *INTERSPEECH*, 2019b.

Kang, L., Riba, P., Wang, Y., Rusiñol, M., Fornés, A., and Villegas, M. Ganwriting: Content-conditioned generation of styled handwritten word images. In *European Conference on Computer Vision (ECCV)*, pp. 273–289. Springer, 2020.

Karras, T., Laine, S., Aittala, M., Hellsten, J., Lehtinen, J., and Aila, T. Analyzing and improving the image quality of StyleGAN. In *IEEE Conference on Computer Vision and Pattern Recognition (CVPR)*, 2020.

Karras, T., Aittala, M., Laine, S., Härkönen, E., Hellsten, J., Lehtinen, J., and Aila, T. Alias-free generative adversarial networks. *Advances in Neural Information Processing Systems (NeurIPS)*, 34, 2021.

Kazemi, H., Iranmanesh, S. M., and Nasrabadi, N. Style and content disentanglement in generative adversarial networks. In *IEEE Winter Conference on Applications of Computer Vision (WACV)*, pp. 848–856, 2019.

Kim, J., Kim, S., Kong, J., and Yoon, S. Glow-TTS: A generative flow for text-to-speech via monotonic alignment search. *Advances in Neural Information Processing Systems (NeurIPS)*, 33, 2020.

Kingma, D. P. and Ba, J. Adam: A method for stochastic optimization. In *International Conference on Learning Representations (ICLR)*, 2015. URL http://arxiv.org/abs/1412.6980.

Kingma, D. P. and Welling, M. Auto-encoding variational bayes. In *International Conference on Learning Representations (ICLR)*, 2014.

Kinnunen, T., Delgado, H., Evans, N., Lee, K. A., Vestman, V., Nautsch, A., Todisco, M., Wang, X., Sahidullah, M., Yamagishi, J., et al. Tandem assessment of spoofing countermeasures and automatic speaker verification: Fundamentals. *IEEE/ACM Transactions on Audio, Speech, and Language Processing*, 28:2195–2210, 2020.

Kotani, A., Tellex, S., and Tompkin, J. Generating handwriting via decoupled style descriptors. In *European Conference on Computer Vision (ECCV)*, pp. 764–780. Springer, 2020.

Kotovenko, D., Sanakoyeu, A., Lang, S., and Ommer, B. Content and style disentanglement for artistic style transfer. In *IEEE International Conference on Computer Vision (ICCV)*, pp. 4422–4431, 2019.

Kwon, G. and Ye, J. C. Diagonal attention and style-based gan for content-style disentanglement in image generation and translation. In *IEEE International Conference on Computer Vision (ICCV)*, pp. 13980–13989, 2021.

Lample, G., Zeghidour, N., Usunier, N., Bordes, A., DENOYER, L., and Ranzato, M. A. Fader networks:manipulating images by sliding attributes. In *Advances in Neural Information Processing Systems (NeurIPS)*, 2017.

Lee, S.-H., Kim, J.-H., Chung, H., and Lee, S.-W. Voicemixer: Adversarial voice style mixup. *Advances in Neural Information Processing Systems (NeurIPS)*, 34, 2021.

Lyu, S. Deepfake detection: Current challenges and next steps. In *2020 IEEE International Conference on Multimedia & Expo Workshops (ICMEW)*, pp. 1–6. IEEE, 2020.

Ma, S., Mcduff, D., and Song, Y. Neural TTS stylization with adversarial and collaborative games. In *International Conference on Learning Representations (ICLR)*, 2018.

McAuliffe, M., Socolof, M., Mihuc, S., Wagner, M., and Sonderegger, M. Montreal forced aligner: Trainable text-speech alignment using kaldi. In *Interspeech*, volume 2017, pp. 498–502, 2017.

Meng, C., Song, J., Song, Y., Zhao, S., and Ermon, S. Improved autoregressive modeling with distribution smoothing. In *International Conference on Learning Representations (ICLR)*, 2021.

Pavllo, D., Lucchi, A., and Hofmann, T. Controlling style and semantics in weakly-supervised image generation. In *European Conference on Computer Vision (ECCV)*, pp. 482–499. Springer, 2020.

Ping, W., Peng, K., Gibiansky, A., Arik, S. Ö., Kannan, A., Narang, S., Raiman, J., and Miller, J. Deep voice 3: Scaling text-to-speech with convolutional sequence learning.

In *International Conference on Learning Representations (ICLR)*, 2018.

Prenger, R., Valle, R., and Catanzaro, B. Waveglow: A flow-based generative network for speech synthesis. In *IEEE International Conference on Acoustics, Speech and Signal Processing(ICASSP)*, pp. 3617–3621. IEEE, 2019.

Qian, K., Zhang, Y., Chang, S., Yang, X., and Hasegawa-Johnson, M. AutoVC: Zero-shot voice style transfer with only autoencoder loss. In *International Conference on Machine Learning (ICML)*, pp. 5210–5219. PMLR, 2019.

Qian, K., Zhang, Y., Chang, S., Hasegawa-Johnson, M., and Cox, D. Unsupervised speech decomposition via triple information bottleneck. In *International Conference on Machine Learning (ICML)*, pp. 7836–7846. PMLR, 2020.

Ramachandran, P., Zoph, B., and Le, Q. Searching for activation functions. In *International Conference on Learning Representations (ICLR)*, 2018.

Ren, Y., Hu, C., Tan, X., Qin, T., Zhao, S., Zhao, Z., and Liu, T.-Y. Fastspeech 2: Fast and high-quality end-to-end text to speech. *arXiv preprint arXiv:2006.04558*, 2020.

Shen, J., Pang, R., Weiss, R. J., Schuster, M., Jaitly, N., Yang, Z., Chen, Z., Zhang, Y., Wang, Y., Skerrv-Ryan, R., et al. Natural TTS synthesis by conditioning waveNet on mel spectrogram predictions. In *IEEE International Conference on Acoustics, Speech and Signal Processing(ICASSP)*, pp. 4779–4783, 2018.

Shen, Y., Gu, J., Tang, X., and Zhou, B. Interpreting the latent space of GANs for semantic face editing. In *IEEE Conference on Computer Vision and Pattern Recognition (CVPR)*, 2020.

Singh, K. K., Ojha, U., and Lee, Y. J. FineGAN: Unsupervised hierarchical disentanglement for fine-grained object generation and discovery. In *IEEE Conference on Computer Vision and Pattern Recognition (CVPR)*, 2019.

Skerry-Ryan, R., Battenberg, E., Xiao, Y., Wang, Y., Stanton, D., Shor, J., Weiss, R., Clark, R., and Saurous, R. A. Towards end-to-end prosody transfer for expressive speech synthesis with tacotron. In *International Conference on Machine Learning (ICML)*, pp. 4693–4702, 2018.

Snyder, D., Garcia-Romero, D., Sell, G., Povey, D., and Khudanpur, S. X-vectors: Robust dnn embeddings for speaker recognition. In *IEEE International Conference on Acoustics, Speech and Signal Processing(ICASSP)*, pp. 5329–5333. IEEE, 2018.

Sun, G., Zhang, Y., Weiss, R. J., Cao, Y., Zen, H., Rosenberg, A., Ramabhadran, B., and Wu, Y. Generating diverse and natural text-to-speech samples using a quantized fine-grained VAE and autoregressive prosody prior. In *IEEE International Conference on Acoustics, Speech and Signal Processing(ICASSP)*, pp. 6699–6703, 2020a.

Sun, G., Zhang, Y., Weiss, R. J., Cao, Y., Zen, H., and Wu, Y. Fully-hierarchical fine-grained prosody modeling for interpretable speech synthesis. In *IEEE International Conference on Acoustics, Speech and Signal Processing(ICASSP)*, pp. 6264–6268. IEEE, 2020b.

Valle, R., Li, J., Prenger, R., and Catanzaro, B. Mellotron: Multispeaker expressive voice synthesis by conditioning on rhythm, pitch and global style tokens. In *IEEE International Conference on Acoustics, Speech and Signal Processing(ICASSP)*, pp. 6189–6193. IEEE, 2020.

Vaswani, A., Shazeer, N., Parmar, N., Uszkoreit, J., Jones, L., Gomez, A. N., Kaiser, L. u., and Polosukhin, I. Attention is all you need. In Guyon, I., Luxburg, U. V., Bengio, S., Wallach, H., Fergus, R., Vishwanathan, S., and Garnett, R. (eds.), *Advances in Neural Information Processing Systems (NeurIPS)*, volume 30. Curran Associates, Inc., 2017. URL https://proceedings.neurips.cc/paper/2017/file/3f5ee243547dee91fbd053c1c4a845aa-Paper.pdf.

Wang, Y., Stanton, D., Zhang, Y., Ryan, R.-S., Battenberg, E., Shor, J., Xiao, Y., Jia, Y., Ren, F., and Saurous, R. A. Style tokens: Unsupervised style modeling, control and transfer in end-to-end speech synthesis. In *International Conference on Machine Learning (ICML)*, pp. 5180–5189. PMLR, 2018.

Wu, Z., Yamagishi, J., Kinnunen, T., Hanilcci, C., Sahidullah, M., Sizov, A., Evans, N., Todisco, M., and Delgado, H. Asvspoof: the automatic speaker verification spoofing and countermeasures challenge. *IEEE Journal of Selected Topics in Signal Processing*, 11(4):588–604, 2017.

Yamagishi, J., Veaux, C., and MacDonald, K. CSTR VCTK Corpus: English Multi-speaker Corpus for CSTR Voice Cloning Toolkit (version 0.92), [sound]. *University of Edinburgh. The Centre for Speech Technology Research (CSTR). https://doi.org/10.7488/ds/2645.*, 2019.

Zen, H., Dang, V., Clark, R., Zhang, Y., Weiss, R. J., Jia, Y., Chen, Z., and Wu, Y. LibriTTS: A corpus derived from librispeech for text-to-speech. *arXiv preprint arXiv:1904.02882*, 2019.

Zhang, R. Making convolutional networks shift-invariant again. In *International Conference on Machine Learning (ICML)*, pp. 7324–7334. PMLR, 2019.

Zhang, Y., Zhang, Y., and Cai, W. Separating style and content for generalized style transfer. In *IEEE Conference*

on Computer Vision and Pattern Recognition (CVPR), pp. 8447–8455, 2018.

Zhao, Y., Huang, W.-C., Tian, X., Yamagishi, J., Das, R. K., Kinnunen, T., Ling, Z., and Toda, T. Voice conversion challenge 2020: Intra-lingual semi-parallel and cross-lingual voice conversion. *arXiv preprint arXiv:2008.12527*, 2020.

Zhu, J.-Y., Park, T., Isola, P., and Efros, A. A. Unpaired image-to-image translation using cycle-consistent adversarial networks. In *IEEE International Conference on Computer Vision (ICCV)*, pp. 2223–2232, 2017.

A. Broader Impact

The technology we develop in the paper, like other artificial intelligence technologies, potentially has both positive and negative impacts to our society (Brundage et al., 2018). One potential risk associated with all generative models is creating fake digital content. If deployed irresponsibly, speech and handwriting synthesis could facilitate deceptive interactions, including mimicking a person's voice or handwriting in automatic speared phishing attacks, gaining security access, or directing public opinions. Examples of responsible deployments of the technology include (but not limited to):

- A system-level authentication every time the technology is used to register style or generate output.

- An encryption system to protect registered style.

- A watermarking system (for both speech and handwriting) such that the generations can be easily identified by human or detection systems (Hua et al., 2016).

Beyond system-level security measures, technologies to identify fake digital content have also been rapidly developed (Chen et al., 2020; Lyu, 2020; Güera & Delp, 2018; Dolhansky et al., 2020; Alegre et al., 2013; Wu et al., 2017; Evans et al., 2013; Kinnunen et al., 2020). Despite the potential negative societal impacts, we believe that the technology will have a larger positive impact, such as enabling new accessibility capabilities (*e.g.*, helping mute people speak in their voices and paralyzed people write in their handwriting) and better human-computer interaction (*e.g.*, by improving downstream speech and handwriting recognizers).

B. Details of the Training Procedure

Training with style equalization is straightforward — we jointly optimize all the model parameters by maximizing the log-likelihood lower bound as described in eq. (1) of the main paper. We found the following optional steps to be useful to improve training and the quality of the generation.

- During training, we found it helpful to add a small amount of Gaussian noise to the ground-truth x_{t-1} that is fed back to the bottom LSTM. Intuitively, we are simulating the noise caused by sampling the output distribution during inference at training time. We found that it makes the inference more stable. A similar method is proposed by Meng et al. (2021) to learn auto-regressive models.

- To encourage the basis A that is used by ϕ in eq. (2) to capture a wide variety of styles, we maintain A as an orthonormal basis. We normalize each column a_i in A to be unit norm in the architecture and minimize $|a_i^\top a_j|^2$ for all i and $j \neq i$. The minimization is conducted by minimizing the trace of $(A^\top A)^2$, which is estimated efficiently using Hutchinson's trace estimator (Hutchinson, 1989) with 100 random samples from a standard Normal distribution. The estimated value is used as a regularization with loss weight equal to 1.

Overall, we optimize the following objective function

$$\max_{\substack{\theta, A}} \underset{\substack{(\mathbf{x},\mathbf{c})\sim\mathcal{X} \\ (\mathbf{x}',\mathbf{c}')\sim\mathcal{X} \\ \mathbf{n}\sim\mathcal{N}(0,\sigma^2)}}{\mathbb{E}} \sum_{t=1}^{M} \underset{z_t\sim q_\theta(z_t|\mathcal{M}_\theta(\mathbf{x}',\phi_\theta(\mathbf{x}',\mathbf{x}),\mathbf{x}_{1..t-1},\mathbf{c})}{\mathbb{E}} \log p_\theta(x_t|z_t, \mathbf{x}_{1..t-1} + \mathbf{n}_{1..t-1}, \mathbf{c})$$

$$- \mathcal{D}_{KL}\left(q_\theta(z_t|\mathcal{M}_\theta(\mathbf{x}',\phi_\theta(\mathbf{x}',\mathbf{x}),\mathbf{x}_{1..t-1},\mathbf{c}) \,||\, p_\theta(z_t|\mathbf{x}_{1..t-1},\mathbf{c})\right) - \mathrm{tr}\left((A^\top A)^2\right), \quad (3)$$

where θ represents all network parameters (except A). We use the reparameterization trick that is commonly used in variational autoencoders (Kingma & Welling, 2014) with one sample to estimate the inner expectation in eq. (3), and we use ADAM (Kingma & Ba, 2015) with $\beta_1 = 0.9$, $\beta_2 = 0.98$, and a learning rate schedule used by Vaswani et al. (2017) with a warm-up period of $4,000$ iterations to optimize the objective function. The learning rate increases rapidly within the warm-up period to 10^{-4} and decreases slowly after then.
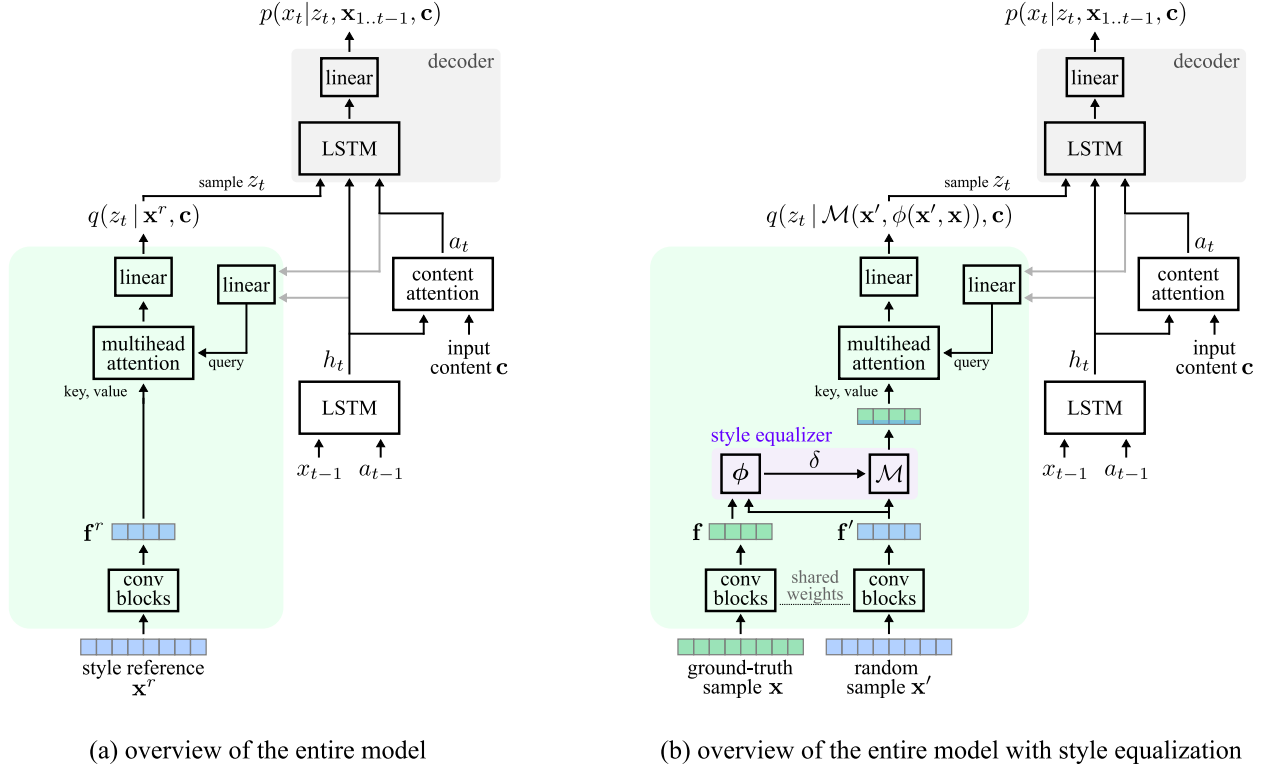
(a) overview of the entire model   (b) overview of the entire model with style equalization

Figure 5: **Overview of the model.** (a) shows an overview of the entire model without style equalization (used during inference since $\delta = \phi(\mathbf{x}^r, \mathbf{x}^r) = 0$). It includes a style encoder (in green), a content attention, a decoder (in gray), and a LSTM at the bottom. Note that the input content $\mathbf{c}$ can be the output of a content-embedding network (used in speech synthesis) or one-hot encoding of characters (used in handwriting synthesis). a_t is the output of the content attention at time t, which is a linear combination of the elements in $\mathbf{c}$. (b) shows an overview of the entire model with style equalization (used during training or during interpolation). ϕ computes the vector δ that encodes the amount of style transformation between $\mathbf{x}'$ and $\mathbf{x}$. $\mathcal{M}$ applies this transformation to $\mathbf{x}'$ to match the style of $\mathbf{x}$. Please see Table 4 for details about individual blocks.

C. Model Architecture Details

In this section, we provide more details about the model architecture used in the paper. Fig. 5 shows an overview of the model, and Table 4 lists the individual block formulations used in Fig. 5. We use the same architecture for both handwriting and speech synthesis, except for the hyper-parameters, which we list at the end of the section.

The model can be separated into a backbone and a style encoder. The backbone is composed of a decoder, content attention, and an LSTM at the bottom. It is a standard model architecture and has been used and extended in many works of handwriting and speech synthesis (Graves, 2013; Shen et al., 2018; Wang et al., 2018; Hsu et al., 2018).

The bottom LSTM is one-layer, and it accumulates information from the past outputs $\mathbf{x}_{1..t-1}$ and the previously attended content $a_1, \ldots, a_{t-1}$ into its hidden state h_t. The content attention, which is proposed by Graves (2013), utilizes moving Gaussian windows to calculate attention weights for the content. The focused content a_t at time t is a linear combination of the elements in $\mathbf{c}$ based on the attention weights. The decoder at the top is a two-layer LSTM that takes all available information, including h_t, z_t, and a_t, and outputs the parameters of $p(x_t|z_t, \mathbf{x}_{1..t-1}, \mathbf{c})$. As mentioned in Sec. B, we add a small Gaussian noise to x_{t-1} that is passed to the bottom LSTM.

Our style encoder is composed of a 4-layer convolutional network and a multi-head attention layer. Given a style reference input $\mathbf{x}^r$, the convolutional network extracts the feature sequence $\mathbf{f}^r$. We apply low-pass filtering before every sub-sampling (Zhang, 2019) to avoid aliasing caused by sub-sampling in the convolutional network. To maintain time-invariant of the convolutional network, we do not add any padding (Islam et al., 2019). Given the past outputs h_t and the currently focused content c_t, we use multi-head attention to extract relevant information from $\mathbf{f}^r$. The query vector is computed

Table 4: Block formulation used in Fig. 5

Block name	Architecture
conv blocks	$\text{blur} \rightarrow \text{conv}(3, f_1, 2, 0) \rightarrow \text{Swish} \rightarrow \text{dropout}(0.1) \rightarrow$
	$\text{blur} \rightarrow \text{conv}(3, f_2, 2, 0) \rightarrow \text{Swish} \rightarrow \text{dropout}(0.1) \rightarrow$
	$\text{blur} \rightarrow \text{conv}(3, f_3, 2, 0) \rightarrow \text{Swish} \rightarrow \text{dropout}(0.1) \rightarrow$
	$\text{blur} \rightarrow \text{conv}(3, f_4, 2, 0) \rightarrow \text{Swish} \rightarrow \text{dropout}(0.1)$
	$(f_1, f_2, f_3, f_4) = \begin{cases} (32, 64, 128, 256), & \text{for handwriting} \\ (256, 384, 512, 512), & \text{for speech} \end{cases}$
multihead attention	number of heads = 4
	$\text{dimension of query, key, value} = \begin{cases} 128, & \text{for handwriting} \\ 64, & \text{for VCTK} \\ 192, & \text{for LibriTTS} \end{cases}$
bottom LSTM	number of layers = 1
	$\text{dimension} = \begin{cases} 512, & \text{for handwriting} \\ 2048, & \text{for speech} \end{cases}$
top LSTM	number of layers = 2
	$\text{dimension} = \begin{cases} 512, & \text{for handwriting} \\ 2048, & \text{for speech} \end{cases}$
content attention	number of Gaussian windows = 10
	See (Graves, 2013) for the exact formulation.
content encoder (speech-only)	$\text{conv}(5, 256, 1, 2) \rightarrow \text{Swish} \rightarrow \text{conv}(5, 256, 1, 2) \rightarrow \text{Swish} \rightarrow$
	$\text{conv}(5, 256, 1, 2) \rightarrow \text{Swish} \rightarrow \text{bidirectional LSTM (dim=256)}$

blur: 1D low-pass filtering with kernel $[1\ 3\ 3\ 1]$
conv(k, f, s, p): 1D convolution with kernel size k, feature dimension f, stride s, and padding p
Swish: Swish nonlinearity (Ramachandran et al., 2018; Hendrycks & Gimpel, 2016)
dropout(p): dropout with probability p

from h_t and c_t using a linear layer, and the key and the value vectors are the individual feature vectors contained in the sequence $\mathbf{f}^r$ without positional encoding. The intuition is that if the model plans to write a specific character or utter a specific word, it should find the information in the style reference and mimic it. The variational approximation $q(z_t|\cdot)$ is a multivariate Gaussian distribution with a diagonal covariance matrix. The prior distribution $p(z_t|\mathbf{x}_{1..t-1}, \mathbf{c})$ is also modeled as a multivariate Gaussian distribution with a diagonal covariance matrix, and we a two-layer feed-forward network to compute its means and standard deviations from h_t and c_t. When the style equalization is used, $\mathcal{M}$ and ϕ are inserted into the style encoder, as shown in Fig. 5(b).

Now we summarize the hyper-parameters used for handwriting and speech. Please also see Table 4.

- For handwriting, the dimension of all LSTMs are 512. The final linear layer outputs a 122-dimensional vector, which is used to parameterize the output distribution. The output distribution includes a mixture of 20 bivariate Gaussian distributions that model the pen movement, a Bernoulli distribution for pen lifting, and a Bernoulli distribution for sequence stops. The posterior and the prior Gaussian distributions are 256-dimensional. The convolutional network in the style encoder has four layers; all of them use kernel size 3, stride 2, and no padding. Their feature dimensions are $3 \rightarrow 32 \rightarrow 64 \rightarrow 128 \rightarrow 256$. We use dropout with a dropping rate equal to 0.1 after each nonlinearity in the convolutional network. The multihead attention has 4 heads, the dimension of the query, key, and value vectors are all 256.

The dimension of δ (*i.e.*, k) is 128. The input content $\mathbf{c}$ is represented as 200-dimensional one-hot vectors of the input characters. The standard deviation of the Gaussian noise is 0.1, and during inference, we reduce the standard deviation of the output distribution to 0.9 of the original one. The model is trained for 100 epochs on a machine with 8 A100 GPUs, and the training took 36 hours.

- For speech, all LSTMs have the same 2048 dimension. The final linear layer outputs a 484-dimensional vector, which is used to parameterize the output distribution. The output distribution includes a mixture of three 80-dimensional Gaussian distributions with diagonal covariance that models the mel-spectrogram and a Bernoulli distribution for sequence stops. The convolutional network in the style encoder has four layers; all of them use kernel size 3, stride 2, no padding. Their feature dimensions are $80 \rightarrow 256 \rightarrow 384 \rightarrow 512 \rightarrow 512$. We use dropout with a dropping rate equal to 0.1 after each nonlinearity in the convolutional network. The multihead attention has 4 heads, the dimension of the query, key, and value vectors are all 256.

  The input sentence is represented as phonemes, which contain 148 symbols. We follow the pre-processing used by Shen et al. (2018) for phoneme and mel-spectrogram extraction. We also follow Shen et al. (2018) and use a bidirectional LSTM and a convolutional network to encode the dependencies between phonemes. The architecture is the same as that used by Shen et al. (2018). The posterior and prior Gaussian distributions are 512-dimensional, and the dimension of δ (*i.e.*, k) is 64 for VCTK dataset and 192 for LibriTTS dataset. The standard deviation of the added noise is 0.2, and during inference, we reduce the standard deviation of the output distribution to 0.74 of the original one. The VCTK model is trained for 70 epochs on a machine with 8 A100 GPUs, and the training took 12 hours; the LibriTTS model is trained for 25 epochs on a machine with 8 A100 GPUs, and the training took 3 days. During inference, the LibriTTS model generates $\sim$380 mel-spectrogram frames (4.4 seconds) per second on a single A100 GPU.

D. Style Classifier Network

As we mentioned in Sec. 5.2, we train a speaker classifier using the objective function proposed by Deng et al. (2019). Using the features extracted by the speaker classifier, we measure the style similarity between two waveforms using the cosine similarity between the features. The style classifier comprises a convolutional network, an LSTM, and a linear layer that transforms the last hidden state into the feature that we use to compute the cosine similarity. The input to the convolutional network is the 80-dimensional phoneme, which is extracted using the same procedure as the one used by Shen et al. (2018). The convolutional network has four layers; all of them use kernel size 3, stride 2, valid padding, and swish non-linearity (Ramachandran et al., 2018). Their feature dimensions are $80 \rightarrow 256 \rightarrow 384 \rightarrow 512 \rightarrow 512$. We use dropout with a dropping rate equal to 0.1 after each non-linearity in the convolutional network. The LSTM has one layer, and its dimension is 512. We split the training set of LibriTTS-all-960 into the training, validation, and test sets by a ratio of 85%, 7.5%, 7.5%, respectively. We use the same learning rate schedule and optimizer mentioned above to train the classifier. The classifier achieves 96.5% validation accuracy.

E. Overview of Related Works

We provide a high-level summary of various controllable sequence generative models in Table 5. In the table, we compare the methods on their needs of : (1) user identification or pretrained embedding, (2) phoneme or character segmentation, (3) content recognizer or pretrained encoder, (4) their training loss and procedure, and (5) the applications shown in the papers. As can be seen and to the best of our knowledge, while there exist many controllable sequence generative models, our proposed method is the first that does not require user ID, segmentation, pretrained recognizer and proven to be applicable on both speech and handwriting domains.

F. Additional Ablation Study: Does $\mathbf{x}'$ Need to be a Valid Sample?

During training, the proposed style equalization randomly selects a sample from the training dataset as $\mathbf{x}'$, which is unrelated to the ground-truth $\mathbf{x}$. One interesting question can be raised naturally: "Since $\mathbf{x}'$ is unrelated to $\mathbf{x}$, do we really need it to be a valid sample?". Theoretically, since our design of $\mathcal{M}$ and ϕ in eq. (2) prevents content leakage and transfers time-independent ground-truth style information from $\mathbf{x}$ through $\mathbf{z}$, as long as $\mathbf{x}'$ does not contain the content information about $\mathbf{x}$, the learned model should be able to control style and content separately during inference. To verify the hypothesis, we conduct the following ablation studies:

Table 5: Overview of controllable sequence models. The table provides a high-level overview of various controllable sequence models. For details, please see individual references.

Method	No user ID or embedding needed	No segmentation needed	No recognizer needed	Training method	Domain
(Kim et al., 2020)	○	●	●	log-likelihood	speech
(Chen et al., 2021)	○	○	●	log-likelihood	speech
(Donahue et al., 2020)	○	●	●	adversarial	speech
(Donahue et al., 2020)	○	●	●	adversarial	speech
(Kameoka et al., 2020)	○	●	●	log-likelihood	speech
(Gibiansky et al., 2017)	○	◗ (pretrained)	●	log-likelihood	speech
(Jia et al., 2018)	○	●	●	log-likelihood	speech
(Skerry-Ryan et al., 2018)	○	●	●	log-likelihood	speech
(Sun et al., 2020a)	○	●	●	log-likelihood	speech
(Lee et al., 2021)	○	●	●	adversarial	speech
(Kaneko et al., 2019b)	○	●	●	adversarial	speech
(Kaneko et al., 2019a)	○ (group data)	●	●	adversarial	speech
(Kaneko & Kameoka, 2018)	○ (group data)	●	●	adversarial	speech
(Kameoka et al., 2018)	○	●	●	adversarial	speech
(Davis et al., 2020)	●	◗ (pretrained)	○	adversarial + log-likelihood	handwriting
(Kang et al., 2020)	○	●	○	adversarial + log-likelihood	handwriting
(Bhunia et al., 2021)	○	●	○	adversarial + log-likelihood	handwriting
(Kotani et al., 2020)	○	◗ (pretrained)	●	log-likelihood	handwriting
(Hsu et al., 2018)	◗ (not on LibriTTS)	●	●	log-likelihood	speech
(Hu et al., 2020)	●	●	◗ (pretrained content encoder)	adversarial + log-likelihood	speech
(Aksan et al., 2018)	●	○	○	log-likelihood	handwriting
(Akuzawa et al., 2018)	●	●	●	log-likelihood + KL-annealing	speech
(Henter et al., 2018)	●	○	●	log-likelihood	speech
(Sun et al., 2020b)	○	○	●	log-likelihood	speech
(Ma et al., 2018)	●	●	●	adversarial	speech
(Graves, 2013)	●	●	●	log-likelihood	handwriting
GST (Wang et al., 2018)	●	●	●	log-likelihood	speech
Proposed style equalization	●	●	●	log-likelihood	speech, handwriting

1. $\mathbf{x}'$ is a fixed vector: We initialize $\mathbf{x}'$ as a random vector but fixed it during training and inference.

2. $\mathbf{x}'$ is a random noise: We randomly sample $\mathbf{x}'$ from the standard Gaussian distribution.

As can be seen from Table 6, both methods are able to produce high-quality models that can control content and style (low WER and `sRank` and high `cos-sim`). They also achieve higher `cos-sim` than GST-nS, which utilizes additional speaker information. Nevertheless, the proposed model (*i.e.*, using real samples as $\mathbf{x}'$) is able to utilize both time-independent and *time-dependent* style information of $\mathbf{x}$ (see discussion in Sec. 5.4), and thus, our model still outperforms the two models.

The following properties also make the proposed method more favorable than the other two cases:

• During inference, the two models still need to run $\mathcal{M}$ and ϕ. In comparison, our usage of $\mathbf{x}'$ allows us to remove $\mathcal{M}$ and ϕ when mimicking a reference example.

• Interpolation between two reference examples becomes non-trivial. By design, using a valid sample as $\mathbf{x}'$ enables the model to learn to transform the style from one real sample to another. In contrast, the other two models only learn to transfer style to a random noise (or a fixed vector).

Table 6: Ablation study results on the role of $\mathbf{x}'$. All models are trained on LibriTTS-all-960 dataset.

Method	Seen speakers, parallel text			Seen speakers, nonparallel text		
	WER (%)	cos-sim ↑	sRank ↓	WER (%)	cos-sim ↑	sRank ↓
$\mathbf{x}'$ is a fixed vector	8.0 ± 0.2	0.69 ± 0.22	14 ± 78	7.1 ± 0.1	0.70 ± 0.20	12 ± 95
$\mathbf{x}'$ is random noise	8.4 ± 0.0	0.72 ± 0.17	4.7 ± 32	$\mathbf{6.7 \pm 0.2}$	0.72 ± 0.16	5.1 ± 56
Proposed ($\mathbf{x}'$ is a real sample)	$\mathbf{6.2 \pm 0.5}$	0.82 ± 0.14	$\mathbf{1.7 \pm 4.1}$	9.4 ± 0.3	0.78 ± 0.14	$\mathbf{1.8 \pm 6.0}$

Method	Unseen speakers, parallel text			Unseen speakers, nonparallel text		
	WER (%)	cos-sim ↑	sRank ↓	WER (%)	cos-sim ↑	sRank ↓
$\mathbf{x}'$ is a fixed vector	9.2 ± 0.3	0.53 ± 0.18	22 ± 97	$\mathbf{6.2 \pm 0.1}$	0.53 ± 0.18	23 ± 103
$\mathbf{x}'$ is random noise	8.9 ± 0.0	0.49 ± 0.16	14 ± 55	6.3 ± 0.2	0.48 ± 0.16	13 ± 56
Proposed ($\mathbf{x}'$ is a real sample)	$\mathbf{6.8 \pm 0.1}$	$\mathbf{0.63 \pm 0.15}$	9.0 ± 63	7.6 ± 0.9	0.57 ± 0.15	$\mathbf{7.4 \pm 43}$

G. Utilizing Time-dependent Style Information

In the section, we try to answer the question: "does our model utilize time-dependent style information?" When a model fully utilizes time-dependent style information, the generated output should be a reconstruction of the reference example in the parallel setting. On the other hand, if a model utilizes only time-independent style information, its outputs in the parallel setting can still be different from the reference example, *i.e.*, the same sentence spoken by the same user can be very different in different contexts. The difference in style replication quality provides the foundation to the following evaluation.

We first evaluate the capability of our model to utilize time-dependent style information by comparing the results between parallel (where all the time-dependent style information is available) and non-parallel (where little time-dependent and mostly time-independent style is available) settings. As can be seen in Table 1, Table 2 and Fig. 3d, our results (WER, CER, and cos-sim) in the parallel setting are better than those in the non-parallel setting. The results show that the model is capable of utilizing the time-dependent information in the reference example.

Next, we verify this capability by visualizing the style attention weights in the three scenarios in Fig. 4b and c. In the parallel setting (Fig. 4b), the model strongly attends to the correct time instance, whereas in the non-parallel setting (Fig. 4c), the model attends to localized pieces in the reference example. Additionally, we invite the readers to qualitatively evaluate the capability via the handwriting/speech generation results provided in the supplemental website. As can be seen, the reproduction is "qualitatively closer" in the parallel setting and in the nonparallel setting when a character appears in the style reference within a similar context, *e.g.*, in Fig. 6b, the character 'A' and 'a' in the first non-parallel text example and 'p' in the second example. To make the observation, in Fig. 6b, we provide a nonparallel example that has overlapping content as the reference style. As can be seen, the generated result is qualitatively similar to the reference example at the overlapped regions even when they are separated by unrelated text.

The ablation study in Table 6 compares our model (which is trained to utilize time-dependent style information via applying style equalization to 50% of the batches) with two models that always transform style inputs (and thus can only use time-independent style information). While all models in the comparison use the same style encoder, our model, with its capability to utilize time-dependent style information, achieves the highest cosine similarities among all three models.

Finally, we compare the same model trained with our method (which applies style equalization to 50% of the batches) and entirely without style equalization in Fig. 3d. While both models can utilize time-dependent information, the model trained without style equalization suffers from content leakage (as shown by the high CER in the nonparallel text setting). In comparison, the proposed model is less effected by the settings.

In summary, the proposed method (utilizing the style attention module and applying style equalization on half of the batches) enables the model to utilize time-dependent style information while avoiding catastrophic content leakage.

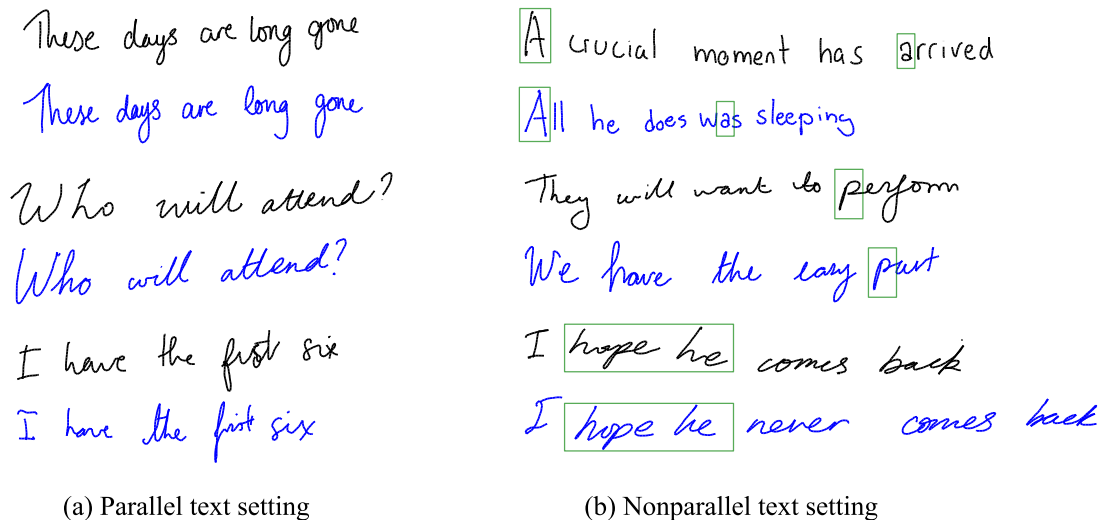(a) Parallel text setting   (b) Nonparallel text setting

Figure 6: Parallel and nonparallel text generation results. In the figure, the reference examples are shown in black, and the generated results are shown in blue.

H. Limitations

Similar to most unsupervised methods, there is no guarantee that the proposed style equalization can *entirely* prevent content leakage, *i.e.* no ground-truth content information contained in the transformed output. The proposed method rely on the time-invariant bottleneck to prevent the ground-truth content information leaking through the transformed style. However, our convolutional network, which is used down-sample the input style examples, has a receptive field equal to 76 mel-spectrogram frames (about 1 second) / handwriting strokes (3 characters) in our models. Within the receptive field, the time-dependent information is retained. In other words, within the receptive field of the convolutional network, our assumption that we only transfer time-invariant information is violated. While we utilize low-pass filtering before any down-sampling and avoid padding as suggested by Zhang (2019), we do not deal with the aliasing due to the nonlinearity functions (as in (Karras et al., 2021)). Thereby, our style transformation is not entirely time-invariant and thus the transformed output can contain time-dependent information exploitable by the model. When the model overfits the training data, our style transform can still leak content information that can eventually be utilized by the decoder. We observe that this phenomenon happens after the model overfits the training set, and by examining the validation loss and the KL-divergence between the prior and the posterior distributions, we can avoid it in practice. As shown by our ablation studies comparing with/without style equalization (Fig. 3a for handwriting and the supplemental webpage for speech), the proposed method effectively reduces content leakage.

I. More Speech and Handwriting Generation Results

On our website (https://apple.github.io/ml-style-equalization), we show an extensive list of speech and handwriting samples generated by the proposed and the baseline methods. Note that it may take a while for the speech results to load, and if the audio players do not contain the play button, please increase the size of the browser window. To remove the effect of the vocoder when comparing synthesized speech samples with real speech samples, all real speech samples (including those in the style opinion score evaluations) are converted to mel-spectrogram and reconstructed back to waveform using the same vocoder that is used by the generative models, *i.e.*, waveglow (Prenger et al., 2019).

For speech synthesis, the webpage contains

- a video showcasing the generation of speech with various styles and content

- nonparallel-text generation with seen speakers from LibriTTS-all-960

- nonparallel-text generation with unseen speakers from LibriTTS-all-960

- an ablation study that compares training with and without style equalization

- interpolation between two unseen style reference speech

- generated speech with random styles sampled from the learned prior

- nonparallel-text generation with seen speakers from VCTK

- parallel-text generation with seen speakers from VCTK

For handwriting synthesis, the webpage contains

- a video showcasing the online generation of handwriting with various styles and content

- nonparallel-text generation with unseen style

- parallel-text generation with unseen style

- generated handwriting with random styles sampled from the learned prior

- interpolation between two unseen style reference handwriting